

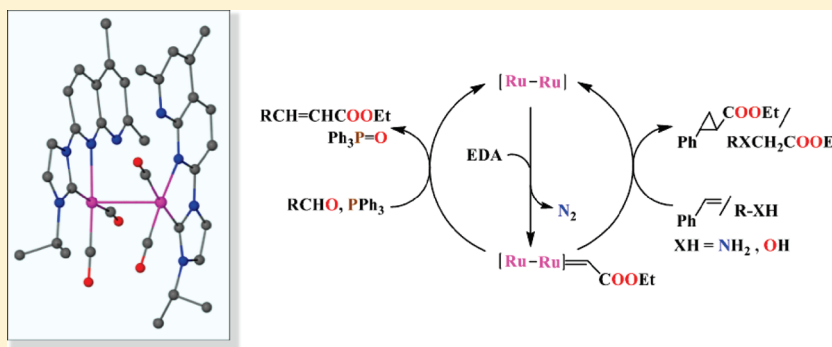
# Site-Directed Anchoring of an N-Heterocyclic Carbene on a Dimetal Platform: Evaluation of a Pair of Diruthenium(I) Catalysts for Carbene-Transfer Reactions from Ethyl Diazoacetate

Biswajit Saha, Tapas Ghatak, Arup Sinha, S. M. Wahidur Rahaman, and Jitendra K. Bera\*

Department of Chemistry, Indian Institute of Technology Kanpur, Kanpur 208016, India

Supporting Information

## ABSTRACT:



Site-directed anchoring of naphthyridine-functionalized N-heterocyclic carbene (NHC) is achieved on a metal–metal singly bonded diruthenium(I) platform. Room-temperature treatment of 1-isopropyl-3-(5,7-dimethyl-1,8-naphthyrid-2-yl)imidazolium bromide (PIN·HBr) with  $\text{Ru}_2(\text{CH}_3\text{COO})_2(\text{CO})_4$  in acetonitrile affords the unsupported compound  $\text{Ru}_2(\text{CO})_4(\kappa^2\text{C}_2\text{N}_1\text{-PIN})_2\text{Br}_2$  (**1**). Judicious alteration in the NHC ligand resulted in the bridged compound  $\text{Ru}_2(\text{CO})_4(\text{CH}_3\text{COO})(\mu^2\text{-}\kappa^2\text{C}_2\text{N}_1\text{-BIN})\text{Br}$  (**2**) (BIN = 1-benzyl-3-(3-phenyl-1,8-naphthyrid-2-yl)imidazol-2-ylidene). X-ray analysis revealed the chelate binding of PIN on each ruthenium at equatorial sites for **1**, and the bridge-chelate binding of BIN spanning the diruthenium core for **2**. The catalytic utilities of the  $\text{BAr}^{\text{F}}$  (tetrakis(3,5-bis(trifluoromethyl)phenyl)borate) salts of these compounds are evaluated toward carbene-transfer reactions from ethyl diazoacetate including aldehyde olefination, cyclopropanation, and X–H (X = O, N) insertions. **1-BAr<sup>F</sup>** is clearly shown to be the superior catalyst. DFT calculations are undertaken to understand the influence of NHC binding on the electronic structures of the “ $\text{Ru}_2(\text{CO})_4$ ” core and to rationalize the lower activity of **2-BAr<sup>F</sup>**.

## INTRODUCTION

The prospect of bimetallic synergy has been largely responsible for the utilization of metal–metal bonded compounds in organometallic catalysis.<sup>1</sup> Several dimetal compounds have gained prominence as catalysts for organic transformations. Incorporation of N-heterocyclic carbene (NHC) is anticipated to boost the catalytic utilities of such compounds.<sup>2</sup> Toward this activity, axial binding of a bare NHC ligand to dirhodium(II) tetracarboxylates and dicobalt hexacarbonyls is reported.<sup>3</sup> Gios et al. have recently demonstrated that the reactivity of dirhodium(II) complexes can be tuned by attaching NHC ligands at sites trans to the Rh–Rh bond.<sup>3b</sup> Equatorial anchoring of NHC on the dimetal core has been achieved by the application of bis-carbene ligands. The bitriazole-2-ylidene (bitz) is shown to form bridged dirhodium complex  $[\text{Rh}_2(\text{bitz})_2(\text{CH}_3\text{CN})_6][\text{BF}_4]_4$  (Scheme 1a).<sup>4</sup> Another variant, 1,1'-methylene-imidazole-2,2'-diylidene, bridges two chromium centers with a short metal–metal distance (Scheme 1b).<sup>5</sup> In both cases, mononuclear chelate complexes were isolated as well. Scrutiny of the current literature indicates an apparent lack of control for the directed synthesis of dimetal–NHC compounds.

We sought to incorporate NHC on dimetal compounds. Site-specific binding of ligands on a dimetal platform affords compounds having well-defined and accessible catalytic sites. Naphthyridine-functionalized NHC ligands were chosen for this purpose owing to their multifaceted coordinating motifs and topological flexibility.<sup>6</sup> Herein we demonstrate the site-directed anchoring of heteroarene-substituted NHC ligands PIN and BIN (Scheme 2) on the metal–metal singly bonded “ $[\text{Ru}_2(\text{CO})_4]$ ” core. The unsupported chelate complex  $\text{Ru}_2(\text{CO})_4(\kappa^2\text{C}_2\text{N}_1\text{-PIN})_2\text{Br}_2$  (**1**) and bridged complex  $\text{Ru}_2(\text{CO})_4(\text{OAc})(\mu^2\text{-}\kappa^2\text{C}_2\text{N}_1\text{-BIN})\text{Br}$  (**2**) are synthesized, and their  $\text{BAr}^{\text{F}}$  (tetrakis(3,5-bis(trifluoromethyl)phenyl)borate) analogues are evaluated as catalysts for carbene-transfer reactions from ethyl diazoacetate (EDA).

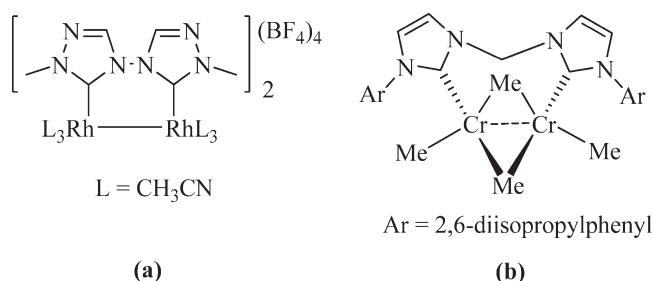
## RESULTS AND DISCUSSION

**Site-Directing Anchoring of NHC.** Room-temperature treatment of the ligand precursor PIN·HBr with  $\text{Ru}_2(\text{CH}_3\text{COO})_2(\text{CO})_4$

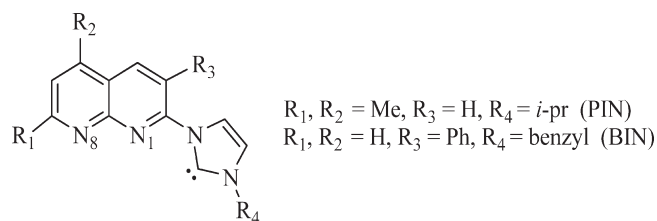
Received: February 15, 2011

Published: March 16, 2011

### Scheme 1. Dimetal Compounds Bridged by bis-NHC Ligands



### Scheme 2. Ligands Employed in This Work



in acetonitrile provides  $\text{Ru}_2(\text{CO})_4(\kappa^2\text{C}_2\text{N}_1\text{-PIN})_2\text{Br}_2$  (**1**). Interestingly, the pyridine analogue 1-mesityl-3-(pyrid-2-yl)imidazolium bromide did not provide the metalated product under identical reaction conditions. The molecular structure of **1** reveals an unsupported diruthenium compound involving two PIN and four carbonyls at equatorial sites (Figure 1). Each ruthenium binds to PIN through its carbene carbon and NP nitrogen, forming a five-membered chelate ring, leaving the other nitrogen uncoordinated. The axial sites are occupied by bromides. The molecule has a crystallographically imposed  $C_2$  symmetry bisecting the Ru–Ru axis. Equatorial PIN and carbonyl ligands adopt a symmetrical anti-staggered conformation about the Ru–Ru bond, making the complex chiral. The Ru–Ru bond length of 2.860(1) Å is marginally longer than the corresponding distance in unsupported bipyridyl (bpy) analogue  $[\text{Ru}_2(\text{bpy})_2(\text{CO})_4(\text{CH}_3\text{CN})_2][\text{PF}_6]_2$  (2.829(1) Å).<sup>7</sup> The Ru–C(carbene) distance is 2.056(9) Å. The carbonyl trans to the carbene carbon makes a longer Ru–C distance (1.921(8) Å) compared to the carbonyl trans to the NP nitrogen (1.841(10) Å). This is an illustration of the stronger trans effect of the carbene carbon in comparison to the arene nitrogen. The  $\text{N}2\text{--Ru}1\text{--Ru}1'\text{--N}2'$  (41.2(4)°) and  $\text{C}23\text{--Ru}1\text{--Ru}1'\text{--C}23'$  (167.6(5)°) torsional angles reflect the staggered orientation of the PIN ligands.

The <sup>1</sup>H NMR spectrum of **1** exhibits a complex pattern indicating the presence of different rotamers in solution.<sup>7,8</sup> The carbene carbon resonates at δ 176.5 ppm in the <sup>13</sup>C NMR spectrum. ESI-MS of **1** exhibits a signal at  $m/z$  947, which is attributed to the species  $[\text{M} - \text{Br} + \text{H}_2\text{O}]^+$ , where M is  $\text{Ru}_2(\text{CO})_4(\text{PIN})_2\text{Br}_2$  (Figure 2a).

The isolation of the chelate complex **1** is intriguing in view of the general tendency of 1,8-naphthyridine (NP) to bridge a variety of dimetal compounds.<sup>9</sup> It was argued that the bridging arrangement of two PIN ligands would have steric repulsion between the ortho substituents.<sup>10</sup> To test this hypothesis, we designed BIN devoid of a substituent at C<sub>7</sub> (Scheme 2). Use of BIN·HBr under similar conditions provided a bridge-chelate complex  $\text{Ru}_2(\text{CO})_4(\text{OAc})(\mu^2\text{-}\kappa^2\text{C}_2\text{N}_1\text{-BIN})\text{Br}$  (**2**). The molecular structure of **2** reveals a

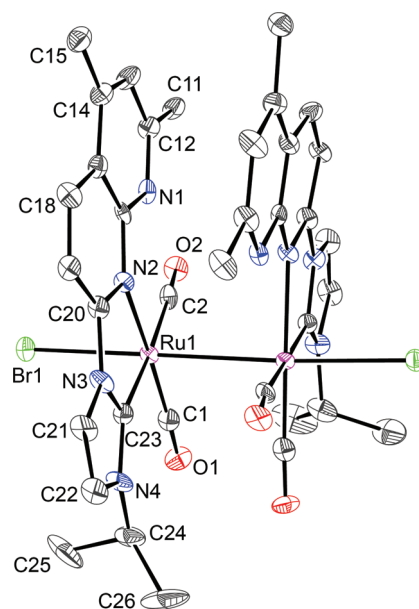


**Figure 1.** ORTEP diagram (40% probability thermal ellipsoids) of **1** with important atoms labeled. Hydrogen atoms are omitted for the sake of clarity. Selected bond lengths (Å) and angles (deg): Ru1–Ru1' 2.860(1), Ru1–C23 2.056(9), Ru1–Br1 2.623(1), Ru1–N2 2.161(1), Ru–C1 1.841(1), Ru–C2 1.921(1), C1–O1 1.158(1), C2–O2 1.145(1), N2–C20 1.351(1), N2–17 1.376(1), N3–C20 1.420(1), N3–C21 1.394(1), N3–C23 1.334(1), N4–C23 1.355(1), N4–C24 1.474(1), C24–C25 1.496(1), C24–C26 1.525(1). Ru1'–Ru1–Br1 176.40(3), Ru1'–Ru1–C23 87.7(3), Ru1'–Ru1–N2 91.2(2), Ru1'–Ru1–C1 87.9(3), Ru1'–Ru1–C2 93.9(3), C23–Ru1–N2 75.7(3), C23–Ru1–C2 175.8(3), C23–Ru1–C1 98.2(4), C2–Ru1–C1 85.8(4), N3–C23–N4 104.5(7). Dihedral angles (deg): N2–Ru1–Ru1'–N2' 41.2(4), C23–Ru1–Ru1'–C23' 167.6(5). Symmetry code:  $-x + 1, -y + 2, z$ .

diruthenium core spanned by one BIN ligand (Figure 3). The NP fragment bridges two ruthenium centers, and the carbene carbon is axially coordinated. The second axial site is occupied by bromide. The diruthenium unit is additionally bridged by one acetate. Two carbonyls are cis oriented to each ruthenium. The Ru1–Ru2 distance of 2.691(1) Å is 0.17 Å shorter than the corresponding distance in the unsupported complex **1**. The Ru–C(carbene) distance of 2.054(4) Å is similar to that observed in **1**.

Incorporation of the second BIN on the diruthenium core could not be achieved. Compound **2** is obtained exclusively even when a 1:1 metal-to-ligand ratio is employed. The <sup>1</sup>H NMR spectrum of **2** is consistent with its solid-state structure. The carbene carbon is observed at δ 170.3 ppm in the <sup>13</sup>C NMR spectrum. ESI-MS exhibits a signal at  $m/z$  737, which is assigned to  $[\text{M} - \text{Br}]^+$ , where M is  $\text{Ru}_2(\text{CO})_4(\text{BIN})(\text{CH}_3\text{COO})\text{Br}$  (Figure 2b).

To understand the effect of NHC anchoring to the diruthenium core, DFT calculations were carried out. For **1**, the naphthyridine and isopropyl groups are replaced by pyridine and hydrogen, respectively, whereas compound **2** is kept unaltered. Geometry optimizations afforded structures that match well with their corresponding X-ray geometries (Figures S1 and S2). Comparison of pertinent metrical parameters reveals slight overestimation at the level of theory employed for this work (Table 1). Although the calculated NPA charges on carbene carbons are similar, the charges on ruthenium atoms are very different. Higher negative charge is computed on Ru (−0.12) in the model complex of **1** than in **2**

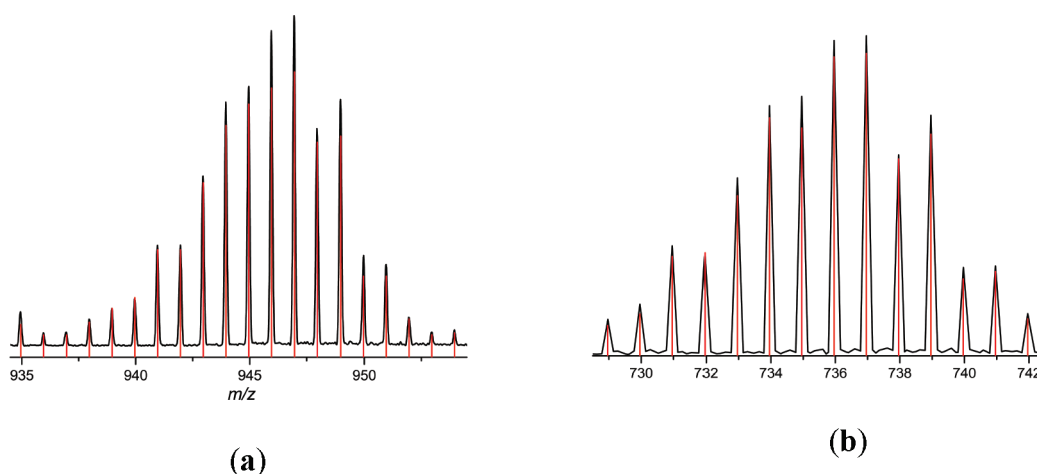


**Figure 2.** Simulated (red line) and experimental mass distributions (black line) for ions  $[M - Br + H_2O]^+$  in **1** (a) and  $[M - Br]^+$  in **2** (b).

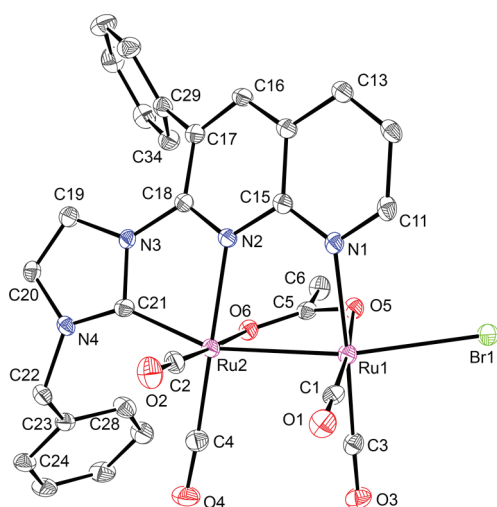


**Figure 3.** ORTEP diagram (40% probability thermal ellipsoids) of **2** with important atoms labeled. Hydrogen atoms are omitted for the sake of clarity. Selected bond lengths (Å) and angles (deg): Ru1–Ru2 2.691(1), Ru1–Br1 2.678(1), Ru1–C1 1.835(4), Ru1–C3 1.854(4), Ru1–N1 2.199(3), Ru1–O5 2.158(2), Ru2–C21 2.054(4), Ru2–C4 1.857(4), Ru2–C2 1.863(4), Ru2–N2 2.156(3), Ru2–O6 2.121(2), C21–N3 1.384(4), C21–N4 1.330(4), N3–C18 1.402(4), N2–C18 1.328(5), N2–C15 1.364(4), N1–C15 1.353(4), N1–C11 1.334(4), C1–O1 1.148(4), C2–O2 1.139(4), C3–O3 1.140(4), C4–O4 1.152(4); Ru2–Ru1–Br1 164.05(1), Ru2–Ru1–N1 84.95(8), Ru2–Ru1–C1 93.46(11), C1–Ru1–Br1 101.73(11), C1–Ru1–O5 175.39(12), C3–Ru1–N1 176.01(13), Ru1–Ru2–C21 157.37(9), N2–Ru2–C21 76.89(12), N2–Ru2–O6 81.16(10), N2–C15–N1 117.6(3). Dihedral angles (deg): C21–Ru2–Ru1–Br1 23.5(2), N2–C18–N3–C21 8.2(4), N1–Ru1–Ru2–C21 44.3(2), N2–Ru2–Ru1–Br1 51.01(9).

(0.00,  $-0.04$ ). Introduction of the second NHC clearly makes the diruthenium core more electron rich in **1**.

Examination of the metal-based orbitals reveals that the axial carbene in **2** destabilizes the Ru–Ru  $\sigma^*$  orbital to a higher extent than **1**, in which the axial ligands are bromides. Contour surfaces of the Ru–Ru  $\sigma^*$  orbitals in the model complex of **1** (LUMO+4) and in **2** (LUMO+6) are shown in Figure 4a and b, respectively. Nonetheless, the destabilization is not reflected in the lengthening of the Ru–Ru distance, which is constrained by the bridging acetate in **2**.

## CARBENE-TRANSFER CATALYSIS

Metal–metal bonded dimetal compounds are excellent catalysts for a wide range of organic transformations.<sup>11</sup> In particular, dirhodium(II) tetracarboxylate and related compounds mediate carbene-transfer reaction from ethyl diazoacetate (EDA) to a variety of substrates.<sup>12</sup> The intermediacy of an electrophilic carbenoid with a linear Rh–Rh–C(carbene) arrangement has been established in this chemistry.<sup>3a–d</sup> The diruthenium(I) complexes **1** and **2** are isoelectronic to the dirhodium(II) systems and offer prospects for axial reactivity. This apparent similarity prompted us to evaluate their catalytic potentials in carbene-transfer reactions.<sup>13</sup> Initial studies with EDA indicated that the axial bromides suppress the reactivity. Hence, these are removed by the application of NaBAR<sup>F</sup> (sodium tetrakis-(3,5-bis(trifluoromethyl)phenyl)borate) in acetonitrile to afford Ru<sub>2</sub>(CO)<sub>4</sub>(PIN)<sub>2</sub>(BAR<sup>F</sup>)<sub>2</sub> (**1-BAR<sup>F</sup>**) and Ru<sub>2</sub>(CO)<sub>4</sub>(CH<sub>3</sub>COO)-(BIN)(BAR<sup>F</sup>) (**2-BAR<sup>F</sup>**), which were characterized by spectroscopic and analytical techniques. The <sup>19</sup>F NMR exhibits signals at  $\delta -62.29$  ppm for **1-BAR<sup>F</sup>** and  $\delta -79.1$  ppm for **2-BAR<sup>F</sup>**. Both compounds have high solubility in common organic solvents, and **1-BAR<sup>F</sup>** is soluble even in diethyl ether. The ylide formation, cyclopropanation, and X–H (X = O, N) insertion reactions are examined (Scheme 3), and the catalytic activities are compared in Table 2.

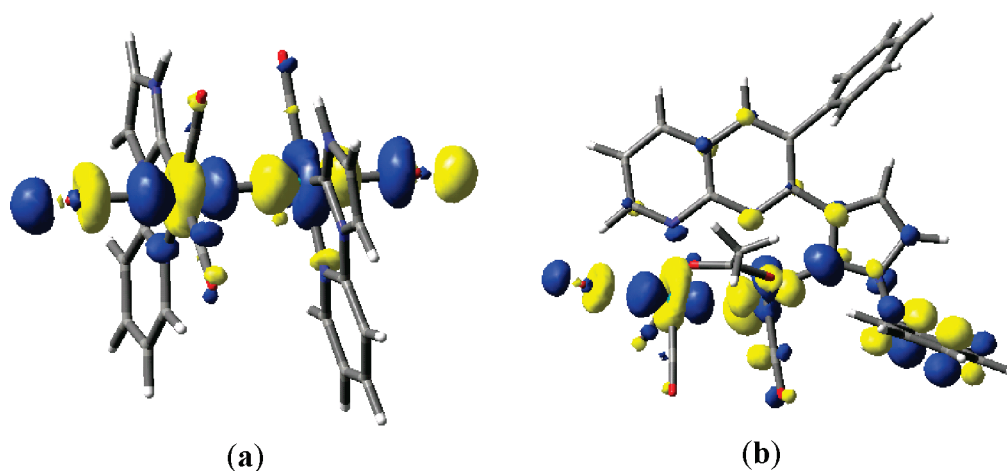
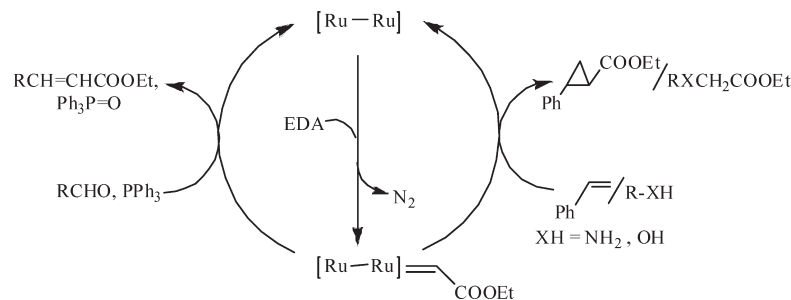
**Aldehyde Olefination.** Aldehyde olefination reaction was carried out using 1.5 mmol of EDA, 1.2 mmol of PPh<sub>3</sub>, and 1 mol % of **1-BAR<sup>F</sup>** as catalyst in toluene. Employment of benzaldehyde in toluene at 80 °C gives ethyl cinnamate in 82% yield after 6 h of reaction time (entry 6). Introduction of an electron-withdrawing nitro group in the aromatic ring led to quantitative conversion for 2,4-dinitrobenzaldehyde in 1 h and for 2-nitro- and 4-nitrobenzaldehydes in 2 h at room temperature with an excellent trans to cis ratio of 99:1 (entries 1–3). 4-Trifluoromethylbenzaldehyde and 4-cyanobenzaldehyde afforded 98% and 93% yields, respectively, after 2 h with high trans selectivity, 97:3 (entries 4 and 5). Electron-rich aldehydes 4-bromo-, 2-hydroxy-, and 4-methylbenzaldehyde afforded lesser yields in the range 74–80% at elevated temperature (80 °C) after 6 h with trans to cis ratio 92:8 (entries 7–9). The least conversion (68%) is observed for electron-rich 4-methoxybenzaldehyde.

Catalyst **2-BAR<sup>F</sup>** affords lesser yields compared to **1-BAR<sup>F</sup>** under similar conditions except for the nitroaldehydes (Table 2). Quantitative conversions of nitro derivatives are observed for both catalysts. Interestingly, though the catalyst **2-BAR<sup>F</sup>** exhibits lesser reactivity, selectivity is not compromised.

**Table 1.** Comparison of Pertinent Metrical Parameters Derived from DFT Calculations,<sup>a</sup> and X-ray and Computed NPA Charges

compound	Ru–Ru (Å)	Ru–C <sub>carbene</sub> (Å)	N–Ru–C (deg)	charge on Ru <sup>c</sup>	charge on C <sub>carbene</sub> <sup>c</sup>
<b>1</b> <sup>b</sup>	2.950 (2.860(1))	2.061 (2.056(9))	75.5 (75.7(3))	−0.12	0.25
<b>2</b>	2.724 (2.691(1))	2.092 (2.054(4))	75.3 (76.9(1))	0.00 −0.04 <sup>d</sup>	0.26

<sup>a</sup>The values in parentheses are from X-ray crystallographic data. <sup>b</sup>A model complex of **1** is used for calculations (see text). <sup>c</sup>Computed NPA charges. <sup>d</sup>Ruthenium bonded to the bromide.

**Figure 4.** Contour surfaces of the Ru–Ru  $\sigma^*$  orbitals in model compound of **1** (LUMO+4) (a) and in **2** (LUMO+6) (b).**Scheme 3.** Carbene-Transfer Catalysis by the Diruthenium(I) Catalyst

The reaction is catalytic since no olefination product was observed without the application of the catalyst. Azine  $\text{O}_2\text{N}-\text{C}_6\text{H}_4-\text{CH}=\text{N}-\text{N}=\text{CH}-\text{CO}_2\text{Et}$  is identified as the only product when 4-nitrobenzaldehyde is reacted with EDA for 36 h in the absence of the catalyst **1-BAr<sup>F</sup>**. The presence of  $\text{PPh}_3$  was found to be essential for this reaction, and no olefination product was observed in its absence (*vide infra*).

**Cyclopropanation.** Room-temperature addition of 1.5 mmol of EDA to a dichloromethane solution of **1-BAr<sup>F</sup>** (0.5 mol %) and olefins (10 mmol) resulted in the formation of the cis and trans cyclopropanes (Scheme 3, Table 2). Dilute EDA solution and excess olefins were added to minimize the dimerization of EDA relative to the desired cyclopropane products. Products were identified by GC and  $^1\text{H}$  NMR, and only isolated yields are reported. Styrene gave a moderate cyclopropanation yield (68%) in 6 h (entry 15). Electron-rich 4-methoxystyrene affords the highest yield (74%) for **1-BAr<sup>F</sup>** (entry 11). Methyl-incorporated styrenes, either on the phenyl ring or at the  $\alpha$ -position, afforded marginally higher yields (entries 12–14) compared to the fluoride derivatives

(entries 16 and 17). The trans to cis ratio in all these cases is 75:25. Cyclopropanation of 1,5-cyclooctadiene and cyclooctene are also achieved by employing this catalyst (entries 18 and 19) albeit in lower yields (58% and 55%, respectively), and the trans to cis ratio is 55:45. Notably, only one double bond is cyclopropanated for 1,5-cyclooctadiene. It should also be noted that the catalyst **1-BAr<sup>F</sup>** affords cyclopropanated products in shorter reaction time and lower catalyst loading compared to  $\text{Ru}_2(\text{CH}_3\text{COO})_2(\text{CO})_4$ .<sup>14</sup>

As observed earlier, catalyst **2-BAr<sup>F</sup>** performs poorly compared to **1-BAr<sup>F</sup>**, affording lesser yields (Table 2) under similar conditions. However, both catalysts exhibit the same selectivity.

**X–H (X = N, O) Insertion.** The insertion of EDA into N–H and O–H bonds is studied with amines and alcohols (Scheme 3). Corresponding amino acid derivatives and ethers were obtained in yields exceeding 80% for **1-BAr<sup>F</sup>** (entries 20–25). In a competing reaction between aniline and styrene, the N–C bonded product is isolated exclusively and no cyclopropane is observed in the GC-MS. Catalyst **1-BAr<sup>F</sup>** affords higher yields than **2-BAr<sup>F</sup>** as reported in earlier cases.

**Table 2. Comparison of Carbene-Transfer Reactions from Ethyl Diazoacetate (EDA) for Catalysts 1-BAr<sup>F</sup> and 2-BAr<sup>F</sup>.**

Entry	Substrate	Product	T (°C)	t (h)	Yield (%)	
					1-BAr <sup>F</sup>	2-BAr <sup>F</sup>
Aldehyde olefination						
$\text{RCHO} + \text{Ph}_3\text{P} + \text{N}_2\text{CHCOOEt} \xrightarrow[1 \text{ mol}\% \text{ Cat. [Ru-Ru]}]{\text{Toluene}} \text{RCH=CHCOOEt} + \text{Ph}_3\text{P=O}$						
1			25	1	100	100
2			25	2	99	99
3			25	2	99	99
4			25	2	98	92
5			25	2	93	89
6			80	6	82	70
7			80	6	79	68
8			80	6	76	67
9			80	6	74	62
10			80	6	68	54
Cyclopropanation						
$\text{RCH=CH}_2 + \text{N}_2\text{CHCOOEt} \xrightarrow[0.5 \text{ mol}\% \text{ Cat. [Ru-Ru]}]{\text{CH}_2\text{Cl}_2} \text{R-CH}_2\text{-CH}_2\text{-COOEt}$						
11			25	6	74	66
12			25	6	72	64
13			25	6	71	62
14			25	6	69	61
15			25	6	68	60
16			25	6	65	58
17			25	6	63	55
18			25	6	58	49
19			25	6	55	46
N–C bond formation						
$\text{RNH}_2 + \text{N}_2\text{CHCOOEt} \xrightarrow[0.5 \text{ mol}\% \text{ Cat. [Ru-Ru]}]{\text{CH}_2\text{Cl}_2} \text{RNHCH}_2\text{COOEt}$						
20			25	6	86	78
21			25	6	85	76
22			25	6	84	72
O–C bond formation						
$\text{ROH} + \text{N}_2\text{CHCOOEt} \xrightarrow[0.5 \text{ mol}\% \text{ Cat. [Ru-Ru]}]{\text{CH}_2\text{Cl}_2} \text{ROCH}_2\text{COOEt}$						
23			25	6	84	76
24			25	6	82	76
25			25	6	81	73

<sup>a</sup> EDA was added slowly to the reaction mixture over a period of 30 min to avoid dimerization. Nevertheless, the dimerized products ethyl maleate and fumarate were observed in a combined yield less than 10% for slow reactions. <sup>b</sup> Aldehyde olefination reaction: 1.5 mmol of EDA in 3 mL of toluene was added slowly to the mixture of 1 mmol of aldehyde, 1.2 mmol of PPh<sub>3</sub>, and 1 mol % 1-BAr<sup>F</sup> or 2-BAr<sup>F</sup> in 5 mL of toluene. <sup>c</sup> Cyclopropanation reaction: 1.5 mmol of EDA in 3 mL of dichloromethane was slowly added to the mixture of 10 mmol of alkene and 0.5 mol % 1-BAr<sup>F</sup> or 2-BAr<sup>F</sup> in 5 mL of dichloromethane. <sup>d</sup> N–H insertion reaction: 1.5 mmol of EDA in 3 mL of dichloromethane was slowly added to the mixture of 1 mmol of amine and 0.5 mol % 1-BAr<sup>F</sup> or 2-BAr<sup>F</sup> in 5 mL of dichloromethane. <sup>e</sup> O–H insertion reaction: 1.5 mmol of EDA in 3 mL of dichloromethane was slowly added to the mixture of 1 mmol of alcohol and 0.5 mol % 1-BAr<sup>F</sup> or 2-BAr<sup>F</sup> in 5 mL of dichloromethane. <sup>f</sup> Isolated yields. For aldehyde olefination and cyclopropanation reactions, combined yields of *E* and *Z* isomers were reported.

The commonality in this set of transformations is the intermediacy of a diruthenium(I) species, [Ru<sup>I</sup>–Ru<sup>I</sup>=CH(COOEt)]. Initially, EDA reacts with the diruthenium catalyst and forms a dimetal-carbenoid intermediate with the extrusion of N<sub>2</sub> (Scheme 3). For the aldehyde olefination reaction, the incipient carbene is transferred to the phosphine, resulting in the phosphorane Ph<sub>3</sub>P=CHCOOEt. In a controlled experiment, the phosphorane was identified by <sup>31</sup>P NMR spectroscopy in the absence of aldehyde.<sup>15</sup> The ylide then reacts with aldehyde to produce the new olefin and phosphine oxide (Scheme S1).<sup>16</sup> The phosphine oxide was identified in the GC-MS. Involvement of the Wittig-type reaction explains the higher reactivity of the electron-deficient aldehydes, which make the carbonyl carbon more electronegative, facilitating the nucleophilic attack of the ylide carbon to aldehyde. It should be pointed out that the diruthenium complex catalyzes the formation of the ylide and not the subsequent Wittig reaction.

For cyclopropanation and N–C and O–C bond formation reactions, the respective substrate alkene, amine, and alcohol directly attack the metal-carbene intermediate and generate the products.

## ■ 1-BAr<sup>F</sup> IS A SUPERIOR CATALYST THAN 2-BAr<sup>F</sup>

1-BAr<sup>F</sup> exhibits superior catalytic activity compared to 2-BAr<sup>F</sup> toward carbene-transfer reactions from EDA. Treatment of either catalyst (0.5 mol %) with EDA in dichloromethane followed by immediate injection of the reaction mixture in GC reveals complete consumption of the diazo compound. Dimers ethyl maleate and ethyl fumarate are the only products observed. It was therefore not possible to ascertain the reactivity difference, as both catalysts rapidly decompose EDA and catalyze the dimer formation. As indicated earlier, these reactions are presumed to proceed via the intermediacy of a diruthenium-carbenoid intermediate. All our attempts to identify such species were not successful. However, to gain insight on their electronic structures, DFT calculations were performed on the model species [1·CHCO<sub>2</sub>Me] (Figure 5a) and [2·CHCO<sub>2</sub>Me] (Figure 5b) (see Experimental Section). As expected, the Ru–Ru distance in unsupported [1·CHCO<sub>2</sub>Me] is longer than in the bridged species [2·CHCO<sub>2</sub>Me]. The Ru–C(carbenoid) distance in [2·CHCO<sub>2</sub>Me] is marginally longer than in [1·CHCO<sub>2</sub>Me], possibly the result of the axial NHC coordination to the second Ru (Table 3). The computed NPA charges are the most revealing. Although NPA charges on Ru bonded to :CHCO<sub>2</sub>Me are similar, carbenoid carbons show very different charges (–0.12 and –0.25). The poor electrophilicity of the carbenoid carbene in 2·CHCO<sub>2</sub>Me, as judged from the computed NPA charge, is attributed to the reduced activity of the catalyst 2-BAr<sup>F</sup>.

One striking difference between catalysts 1 and 2 is that the former has two potential catalytic sites, whereas the latter offers only one axial site. It is, however, unlikely that both axial sites are utilized for catalyst 1-BAr<sup>F</sup>. We earlier demonstrated that the “Ru<sub>2</sub>(CO)<sub>4</sub>” core cleaves the aromatic C–H bond at one of the axial sites to form a cyclometalated product, and the second cyclometalation does not occur even at higher temperature.<sup>17</sup> It is proposed that the formation of the [Ru–Ru]=CHCO<sub>2</sub>Et adduct lowers the electrophilicity of the second Ru, and hence the possibility of the formation of the bis-carbene adduct is greatly diminished. The higher negative charge on the second Ru (–0.16) (Table 3) in 1·CHCO<sub>2</sub>Me supports this assertion. We therefore conclude that the greater reactivity of 1-BAr<sup>F</sup> is due to the higher electrophilicity of the carbenoid carbon and not because of the additional reaction site.

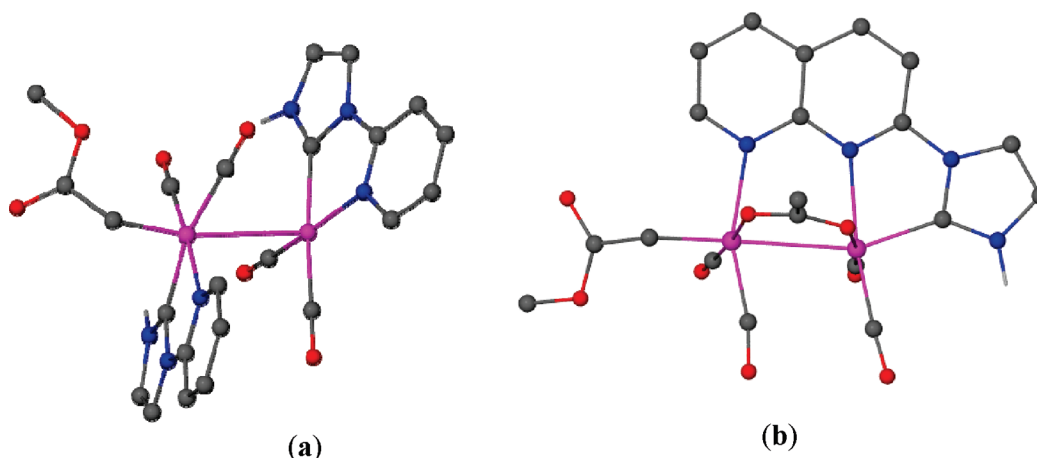


Figure 5. DFT-optimized structures of **1** · CHCO<sub>2</sub>Me (a) and **2** · CHCO<sub>2</sub>Me (b).

Table 3. Pertinent Metrical Parameters<sup>a</sup> and Computed NPA Charges of **1** · CHCO<sub>2</sub>Me and **2** · CHCO<sub>2</sub>Me

species	Ru–Ru (Å)	Ru–C <sup>b</sup> (Å)	Ru	C <sup>b</sup>
<b>1</b> · CHCO <sub>2</sub> Me	2.975	1.925	0.03 <sup>c</sup>	−0.12
			−0.16 <sup>d</sup>	
<b>2</b> · CHCO <sub>2</sub> Me	2.825	1.942	0.01 <sup>c</sup>	−0.25
			0.08 <sup>d</sup>	

<sup>a</sup> Values are from DFT-optimized structures. <sup>b</sup> Carbenoid carbon. <sup>c</sup> NPA charge on ruthenium bonded to the carbenoid carbon. <sup>d</sup> The second Ru.

## CONCLUSION

We herein report the successful incorporation of heteroarene-functionalized NHC on a singly bonded diruthenium(I) compound. Application of naphthyridine-appended NHC (NP-NHC) affords the unsupported compound **1** in high yield. A subtle variation in the ligand framework results in the bridged compound **2** exclusively. Strongly bound NP-NHC and ancillary carbonyls offer prospects for site-specific (axial) reactivity. The **BAR<sup>F</sup>** analogues of these complexes are demonstrated to be excellent catalysts for carbene-transfer reactions from EDA to a variety of substrates. Ylide formation, cyclopropanation, and X–H (X = O, N) insertion reactions highlight the versatility of these catalysts. **1-BAR<sup>F</sup>** is proven to be the superior catalyst and offers a potential alternative to the expensive dirhodium(II) congeners. Efforts are ongoing to develop the chiral versions for asymmetric transformations.

## EXPERIMENTAL SECTION

**General Procedures.** All reactions with metal complexes were carried out under an atmosphere of purified nitrogen using standard Schlenk-vessel and vacuum-line techniques. Infrared spectra were recorded in the range 4000–400 cm<sup>−1</sup> on a Vertex 70 Bruker spectrophotometer on KBr pellets. <sup>1</sup>H NMR spectra were obtained on a JEOL JNM-LA 500 MHz spectrometer. <sup>1</sup>H NMR chemical shifts were referenced to the residual hydrogen signal of the deuterated solvents. Elemental analyses were performed on a Thermoquest EA1110 CHNS/O analyzer. GC-MS experiment was performed on an Agilent 7890A GC and 5975C MS system. The recrystallized compounds were powdered, washed several times with dry diethyl ether or hexane, and dried under vacuum for at least 48 h prior to elemental analyses.

**Materials.** Solvents were dried by conventional methods, distilled under nitrogen, and deoxygenated prior to use. RuCl<sub>3</sub> · *n*H<sub>2</sub>O (39% Ru) was purchased from Arora Matthey, India. The compound [Ru<sub>2</sub>(CH<sub>3</sub>COO)<sub>2</sub>(CO)<sub>4</sub>]<sup>18</sup>

and 2-chloro-1,8-naphthyridine were synthesized following the literature procedures.<sup>6d</sup>

**Synthesis of 1:** The ligand precursor PIN · HBr (125 mg, 0.36 mmol) was added to an acetonitrile solution of [Ru<sub>2</sub>(CH<sub>3</sub>COO)<sub>2</sub>(CO)<sub>4</sub>] (75 mg, 0.17 mmol). The mixture was stirred at room temperature for 48 h. The red solution was concentrated under reduced pressure, and diethyl ether was added to induce precipitation. The red precipitate was washed with diethyl ether and dried under vacuum. Crystals suitable for X-ray diffraction were grown by layering diethyl ether over a concentrated acetonitrile solution of **1** inside an 8 mm o.d. vacuum-sealed glass tube. Yield: 150 mg (86%). <sup>1</sup>H NMR (500 MHz, CD<sub>3</sub>CN, 294 K): δ 9.00–8.84 (m, 1H, NP), 8.26 (d, *J* = 4.0 Hz, 1H, Im), 8.15–8.01 (m, 1H, NP), 7.66–7.64 (m, 1H, NP), 7.53 (d, *J* = 2.1 Hz, 1H, Im), 2.83–2.74 (m, 6H, NP), 1.66–1.46 (m, 6H, iPr). <sup>13</sup>C NMR (125.8 MHz, CD<sub>3</sub>CN, 296.2 K): δ 207.1 (CO), 202.7 (CO), 198.5 (CO), 196.6 (CO), 176.5 (NCN<sub>Im</sub>), 164.4 (CCN<sub>NP</sub>), 154.2 (N<sub>NP</sub>CN<sub>Im</sub>), 148.5 (CCN<sub>NP</sub>), 146.4 (CCC<sub>NP</sub>), 138.4 (CCC<sub>NP</sub>), 138.1 (CCC<sub>NP</sub>), 129.8 (CCC<sub>NP</sub>), 123.7 (NCC<sub>Im</sub>), 120.2 (CCC<sub>NP</sub>), 111.6 (N<sub>Im</sub>CC), 54.4 (CH<sup>iPr</sup>), 24.7 (CH<sub>3</sub><sup>NP</sup>), 22.8 (CH<sub>3</sub><sup>iPr</sup>), 22.1 (CH<sub>3</sub><sup>iPr</sup>), 17.3 (CH<sub>3</sub><sup>NP</sup>). IR (KBr, cm<sup>−1</sup>): ν(CO) 2058, 1992, 1970, 1926. Anal. Calcd for C<sub>36</sub>H<sub>38</sub>N<sub>8</sub>O<sub>4</sub>Br<sub>2</sub>Ru<sub>2</sub>: C, 42.87; H, 3.80; N, 11.11. Found: C, 42.75; H, 3.77; N, 11.02. ESI-MS, *m/z* 947 corresponding to [M – Br + H<sub>2</sub>O]<sup>+</sup> where M is Ru<sub>2</sub>(CO)<sub>4</sub>(PIN)<sub>2</sub>Br<sub>2</sub>.

**Synthesis of 2:** The compound was synthesized following a similar procedure employed for the synthesis of **1** using ligand precursor BIN · HBr (44 mg, 0.1 mmol) and [Ru<sub>2</sub>(CH<sub>3</sub>COO)<sub>2</sub>(CO)<sub>4</sub>] (41 mg, 0.09 mmol) in acetonitrile and stirring for 12 h. Crystals suitable for X-ray diffraction were grown by layering hexane over a concentrated dichloromethane solution of **2** inside an 8 mm o.d. vacuum-sealed glass tube. Yield: 70 mg (90%). <sup>1</sup>H NMR (500 MHz, CD<sub>3</sub>CN, 294 K): δ 8.62 (s, 1H NP), 7.80 (dd, *J* = 12.3, 3.9 Hz, 1H, NP), 7.62 (m, 5H Ph), 7.39 (m, 2H, NP), 7.02 (d, *J* = 2.9 Hz, 1H, Im), 6.47 (d, *J* = 1.9 Hz, 1H Im), 5.62 (d, *J* = 15.7 Hz, 1H, CH<sub>2</sub>), 5.50 (d, *J* = 15.7 Hz, 1H, CH<sub>2</sub>), 1.61 (s, 3H, CH<sub>3</sub>). <sup>13</sup>C NMR (125.8 MHz, CD<sub>3</sub>CN, 296.2 K): δ 203.3 (CO), 201.9 (CO), 197.8 (CO), 196.4 (CO), 170.3 (NCN<sub>Im</sub>), 155.1 (NCN<sub>NP</sub>), 152.7 (NCC<sub>NP</sub>), 146.2 (NCC<sub>NP</sub>), 140.6 (CCC<sub>NP</sub>), 140.1 (CCC<sub>NP</sub>), 138.1 (CCC<sub>NP</sub>), 136.2 (CCC<sub>NP</sub>), 135.6 (CCC<sub>NP</sub>), 129.1 (CCC<sub>Ph</sub>), 127.9 (CCC<sub>Bn</sub>), 128.9 (CCC<sub>Ph</sub>), 127.9 (CCC<sub>Bn</sub>), 128.5 (CCC<sub>Ph</sub>), 129.0 (CCC<sub>Ph</sub>), 128.2 (CCC<sub>Bn</sub>), 127.6 (CCC<sub>Bn</sub>), 123.8 (NCC<sub>Im</sub>), 111.5 (NCN<sub>Im</sub>), 65.4 (OCO<sub>OAc</sub>), 54.9 (CCO<sub>OAc</sub>), 54.4 (CH<sub>2</sub><sup>Bn</sup>). IR (KBr, cm<sup>−1</sup>): ν(CO) 2029, 1959, ν(OAc) 1432. Anal. Calcd for C<sub>30</sub>H<sub>21</sub>N<sub>4</sub>O<sub>6</sub>BrRu<sub>2</sub>: C, 44.18; H, 2.60; N, 6.87. Found: C, 44.12; H, 2.52; N, 6.81. ESI-MS, *m/z* 737 corresponds to [M – Br]<sup>+</sup> where M is Ru<sub>2</sub>(CO)<sub>4</sub>(BIN)(CH<sub>3</sub>COO)Br.

**Synthesis of 1-BAR<sup>F</sup>:** NaBAR<sup>F</sup> (73 mg, 0.08 mmol) was added to an acetonitrile solution of **1** (40 mg, 0.04 mmol). The mixture was stirred at room temperature for 4 h. NaBr was filtered off, and the solvent was removed

completely under reduced pressure. The solid residue was again dissolved in a minimum amount of dichloromethane. Hexane was added to induce precipitation. The red solid was washed with hexane and dried under vacuum. Yield: 96 mg (90%).  $^1\text{H NMR}$  (500 MHz,  $\text{CDCl}_3$ , 294 K):  $\delta$  8.62 (s, 1H NP), 7.80 (dd,  $J = 12.3, 3.9$  Hz, 1H, NP), 7.62 (m, 5H Ph), 7.39 (m, 2H, NP, 5H, Ph), 7.02 (d,  $J = 2.9$  Hz, 1H, Im), 6.47 (d,  $J = 1.9$  Hz, 1H Im), 5.62 (d,  $J = 15.7$  Hz, 1H,  $\text{CH}_2$ ), 5.50 (d,  $J = 15.7$  Hz, 1H,  $\text{CH}_2$ ), 1.61 (s, 3H,  $\text{CH}_3$ ).  $^{13}\text{C NMR}$  (125.8 MHz,  $\text{CDCl}_3$ , 296.2 K):  $\delta$  207.3 (CO), 202.1 (CO), 198.0 (CO), 196.0 (CO) 175.0 (NCN<sub>Imdz</sub>), 166.9 (NCC<sub>NP</sub>), 162.9 (q,  $J_{\text{B,C}} = 50.1$ , C<sub>BAR</sub><sup>F</sup>), 154.1 (N<sub>NP</sub>CN<sub>Imdz</sub>), 146.7 (CCC<sub>NP</sub>), 134.8 (C<sub>BAR</sub><sup>F</sup>), 131.6 (CCC<sub>NP</sub>), 128.9 (qq, C<sub>BAR</sub><sup>F</sup>), 125.8 (C<sub>BAR</sub><sup>F</sup>), 121.3 (NCC<sub>Imdz</sub>), 119.2 (CCC<sub>NP</sub>), 117.6 (C<sub>BAR</sub><sup>F</sup>), 109.1 (N<sub>Im</sub>CC), 55.4 (CCC<sub>NP</sub>), 26.0 (CH<sub>3NP</sub>), 25.9 (CH<sub>3NP</sub>), 22.8 (CH<sub>3</sub>), 17.9 (CH<sub>3NP</sub>).  $^{19}\text{F NMR}$  (470.6 MHz,  $\text{CDCl}_3$ , 292 K):  $\delta$  -62.29. IR (KBr,  $\text{cm}^{-1}$ ):  $\nu$  (CO) 2068, 1998. Anal. Calcd for  $\text{C}_{100}\text{H}_{60}\text{N}_8\text{O}_4\text{B}_2\text{F}_{48}\text{Ru}_2$ : C, 46.67; H, 2.35; N, 4.35. Found: C, 46.61; H, 2.29; N, 4.31.

Synthesis of 2-BAR<sup>F</sup>: NaBAR<sup>F</sup> (43 mg, 0.05 mmol) was added to an acetonitrile solution of 2 (40 mg, 0.05 mmol). The mixture was stirred at room temperature for 4 h. NaBr was filtered off, and the solvent was removed completely under reduced pressure. The solid residue was again dissolved in a minimum amount of dichloromethane. Hexane was added to induce precipitation. The red solid was washed with hexane and dried under vacuum. Yield: 80 mg (90%).  $^1\text{H NMR}$  (500 MHz,  $\text{CDCl}_3$ , 292 K):  $\delta$  8.62 (s, 1H NP), 7.80 (dd,  $J = 12.3, 3.9$  Hz, 1H, NP), 7.62 (m, 5H Ph), 7.39 (m, 2H, NP), 7.02 (d,  $J = 2.9$  Hz, 1H, Im), 6.47 (d,  $J = 1.9$  Hz, 1H Im), 5.62 (d,  $J = 15.7$  Hz, 1H,  $\text{CH}_2$ ), 5.50 (d,  $J = 15.7$  Hz, 1H,  $\text{CH}_2$ ), 1.61 (s, 3H,  $\text{CH}_3$ ).  $^{13}\text{C NMR}$  (125.8 MHz,  $\text{CD}_3\text{CN}$ , 296.2 K):  $\delta$  202.7 (CO), 201.6 (CO), 197.4 (CO), 196.0 (CO) 171.8 (NCN<sub>Im</sub>), 162.1 (q,  $J_{\text{B,C}} = 48.1$ , C<sub>BAR</sub><sup>F</sup>), 156.3 (NCN<sub>NP</sub>), 153.2 (NCC<sub>NP</sub>), 152.7 (NCC<sub>NP</sub>), 150.4 (CCC<sub>NP</sub>), 147.3 (CCC<sub>NP</sub>), 144.7 (CCC<sub>NP</sub>), 144.3 (CCC<sub>NP</sub>), 143.8 (CCC<sub>NP</sub>), 138.9 (C<sub>BAR</sub><sup>F</sup>), 136.1 (CCC<sub>Ph</sub>), 135.4 (CCC<sub>Bn</sub>), 134.9 (CCC<sub>Ph</sub>), 134.2 (CCC<sub>Bn</sub>), 131.5 (CCC<sub>Ph</sub>), 130.2 (CCC<sub>Ph</sub>), 129.5 (CCC<sub>Bn</sub>), 128.1 (qq, C<sub>BAR</sub><sup>F</sup>), 127.4 (CCC<sub>Bn</sub>), 125.4 (NCC<sub>Im</sub>), 124.1 (C<sub>BAR</sub><sup>F</sup>), 117.8 (CCN<sub>Im</sub>), 116.1 (C<sub>BAR</sub><sup>F</sup>), 55.2 (OCO<sub>OAc</sub>), 54.2 (CCO<sub>OAc</sub>), 51.6 (CH<sub>2</sub><sup>Bn</sup>).  $^{19}\text{F NMR}$  (470.6 MHz,  $\text{CD}_3\text{CN}$ , 292 K):  $\delta$  -79.1. IR (KBr,  $\text{cm}^{-1}$ ):  $\nu$  (CO) 2027, 1970,  $\nu$  (OAc) 1435. Anal. Calcd for  $\text{C}_{64}\text{H}_{33}\text{N}_4\text{O}_6\text{BF}_{24}\text{Ru}_2$ : C, 46.37; H, 2.05; N, 3.45. Found: C, 46.31; H, 1.99; N, 3.35.

**X-ray Data Collection and Refinement.** Single-crystal X-ray studies were performed on a CCD Bruker SMART APEX diffractometer equipped with an Oxford Instruments low-temperature attachment. All the data were collected at 100(2) K using graphite-monochromated Mo  $K\alpha$  radiation ( $\lambda = 0.71073$  Å). The frames were indexed, integrated, and scaled using the SMART and SAINT software packages,<sup>19</sup> and the data were corrected for absorption using the SADABS program.<sup>20</sup> The structures were solved and refined with the SHELX suite of programs.<sup>21</sup> All hydrogen atoms were included in the final stages of the refinement and were refined with a typical riding model. Structure solution and refinement details for compounds 1 and 2 are provided in the Supporting Information. All non-hydrogen atoms of compound 1, except C21, C22, and O2, were refined with anisotropic thermal parameters. Anisotropic treatment of these three atoms resulted in nonpositive definite displacement tensors and were therefore subjected to isotropic refinement. All non-hydrogen atoms of compound 2 were refined with anisotropic thermal parameters. The "SQUEEZE" option in PLATON program 22 was used to remove a disordered solvent molecule from the overall intensity data of compound 2. Pertinent crystallographic data for compounds 1 and 2 are summarized in Table 4. ORTEP-32<sup>23</sup> was used to produce the diagrams. CCDC-790978 (1) and -790979 (2) contain the supplementary crystallographic data for this paper. These data can be obtained free of charge from the Cambridge Crystallographic Data Centre via [www.ccdc.cam.ac.uk/data\\_request/cif](http://www.ccdc.cam.ac.uk/data_request/cif).

**Theoretical Study.** Calculations were performed using density functional theory (DFT) with Becke's three-parameter hybrid exchange functional<sup>24</sup> and the Lee–Yang–Parr correlation functional (B3LYP).<sup>25</sup> [ $\mathbf{1} \cdot \text{CHCO}_2\text{Me}$ ] and [ $\mathbf{2} \cdot \text{CHCO}_2\text{Me}$ ] are described for [ $\text{Ru}_2(\text{CO})_4$

**Table 4. Crystallographic Data and Pertinent Refinement Parameters for 1 and 2**

	1	2
empirical formula	$\text{C}_{36}\text{H}_{36}\text{Br}_2\text{N}_8\text{O}_4\text{Ru}_2$	$\text{C}_{30}\text{H}_{21}\text{BrN}_4\text{O}_6\text{Ru}_2$
fw	1006.69	815.56
cryst syst	orthorhombic	monoclinic
space group	$P2(1)2(1)2$	$C2/c$
<i>a</i> (Å)	13.619(3)	26.344(7)
<i>b</i> (Å)	10.350(3)	19.940(6)
<i>c</i> (Å)	13.132(3)	13.903(4)
$\alpha$ (deg)		90.00
$\beta$ (deg)	90.00	121.345(4)
$\gamma$ (deg)		90.00
<i>V</i> (Å <sup>3</sup> )	1851.1(8)	6237(3)
<i>Z</i>	2	8
$\rho_{\text{calcd}}$ (g cm <sup>-3</sup> )	1.806	1.737
$\mu$ (mm <sup>-1</sup> )	3.026	2.297
<i>F</i> (000)	996	3200
reflns collected	12 366	27 242
indep reflns	3139	7643
obsd reflns [ $I > 2\sigma(I)$ ]	2489	6170
no. of variables	224	389
Goof	1.070	1.091
<i>R</i> <sub>int</sub>	0.0638	0.0351
final <i>R</i> indices		
[ $I > 2\sigma(I)$ ] <sup>a</sup>	<i>R</i> 1 = 0.0563 <i>wR</i> 2 = 0.1462	<i>R</i> 1 = 0.0387 <i>wR</i> 2 = 0.0970
<i>R</i> indices (all data) <sup>a</sup>	<i>R</i> 1 = 0.0742 <i>wR</i> 2 = 0.1616	<i>R</i> 1 = 0.0504 <i>wR</i> 2 = 0.1080

$$^a R1 = \sum ||F_o| - |F_c|| / \sum |F_o| \text{ with } F_o^2 > 2\sigma(F_o^2). \quad wR2 = [\sum w(|F_o^2| - |F_c^2|)^2 / \sum |F_o^2|]^2 / 2$$

(pynhc)<sub>2</sub>(CHCO<sub>2</sub>Me)]<sup>2+</sup> and [ $\text{Ru}_2(\text{CO})_4(\text{np-nhc})(\text{CH}_3\text{COO})(\text{CHCO}_2\text{Me})$ ]<sup>+</sup>, respectively, where py-nhc is pyridylimidazol-2-ylidene and np-nhc is 1,8-naphthyridylimidazol-2-ylidene (Figure Sb). Geometry-optimized structures were characterized fully via analytical frequency calculations as minima on the potential energy surface. The double- $\zeta$  basis set of Hay and Wadt (LanL2DZ) with a small core (1s2s2p3s3p3d4s4p4d) effective core potential (ECP)<sup>26</sup> was used for Ru. The ligand atoms H, N, C, and O atoms were described using the 6-31G(d,p) basis sets, and 6-311++G (3df, 3pd) basis sets for the Br atom were employed. All calculations were performed with the Gaussian 03 (G03)<sup>27</sup> suite of programs. Gaussview 3.0 was used for generating the orbital plots. Atomic charges were calculated by natural population analysis (NPA) as implemented in Gaussian 03.<sup>28</sup>

## ■ ASSOCIATED CONTENT

Supporting Information. This material is available free of charge via the Internet at <http://pubs.acs.org>.

## ■ AUTHOR INFORMATION

### Corresponding Author

\*E-mail: [jbera@iitk.ac.in](mailto:jbera@iitk.ac.in).

## ■ ACKNOWLEDGMENT

This work is financially supported by the Department of Science and Technology (DST), India, and Indo-French Centre

for the Promotion of Advanced Research (IFCPAR). J.K.B. thanks DST for the Swarnajayanti fellowship. B.S. and A.S. thank CSIR, and T.G. and W.R. thank UGC, India, for fellowships.

## DEDICATION

Dedicated to Professor Yashwant D. Vankar on the occasion of his 60th birthday.

## REFERENCES

- (1) (a) *Multimetallic Catalysis in Organic Synthesis*; Shibasaki, M.; Yamamoto, Y., Eds.; Wiley-VCH: Weinheim, 2004. (b) Adams, R. A.; Cotton, F. A. *Catalysis by Di- and Polynuclear Metal Cluster Complexes*; Wiley-VCH: New York, 1998. (c) Gambarotta, S.; Scott, J. *Angew. Chem., Int. Ed.* **2004**, *43*, 5298. (d) Sinfelt, H. J. *Acc. Chem. Res.* **1977**, *10*, 15. (e) Adams, R. D.; Captain, B. *Angew. Chem., Int. Ed.* **2008**, *47*, 252. (f) Broussard, M. E.; Juma, B.; Train, S. G.; Peng, W.-J.; Laneman, S. A.; Stanley, G. G. *Science* **1993**, *260*, 1784.
- (2) (a) Nolan, S. P. *N-Heterocyclic Carbenes in Synthesis*; Wiley-VCH Verlag GmbH & Co. KGaA: Weinheim, 2006; and references therein. (b) *N-Heterocyclic Carbenes in Transition Metal Catalysis*; Glorius, F., Ed.; *Topics in Organometallic Chemistry*, 21; Springer: Berlin, 2007. (c) Crabtree, R. H. *J. Organomet. Chem.* **2005**, *690*, 5451. (d) Hahn, F. E.; Jahnke, M. C. *Angew. Chem., Int. Ed.* **2008**, *47*, 3122. (e) Boyd, P. D. W.; Edwards, A. J.; Gardiner, M. G.; Ho, C. C.; Lemée-Cailleau, M.-H.; McGuinness, D. S.; Riapanitra, A.; Steed, J. W.; Stringer, D. N.; Yates, B. F. *Angew. Chem., Int. Ed.* **2010**, *49*, 6315. (f) Diebolt, O.; Braunstein, P.; Nolan, S. P.; Cazin, C. S. J. *Chem. Commun.* **2008**, 3190. (g) Poyatos, M.; Mata, J. A.; Peris, E. *Chem. Rev.* **2009**, *109*, 3677.
- (3) (a) Snyder, J. P.; Padwa, A.; Stengel, T.; Arduengo, A. J., III; Jockisch, A.; Kim, H.-J. *J. Am. Chem. Soc.* **2001**, *123*, 11318. (b) Gois, P. M. P.; Trindade, A. F.; Veiros, L. F.; André, V.; Duarte, M. T.; Afonso, C. A. M.; Caddick, S.; Cloke, F. G. N. *Angew. Chem., Int. Ed.* **2007**, *46*, 5750. (c) Na, S. J.; Lee, B. Y.; Bui, N.-N.; Mho, S.-i.; Jang, H.-Y. *J. Organomet. Chem.* **2007**, *692*, 5523. (d) Trindade, A. F.; Gois, P. M. P.; Veiros, L. F.; André, V.; Duarte, M. T.; Afonso, C. A. M.; Caddick, S.; Cloke, F. G. N. *J. Org. Chem.* **2008**, *73*, 4076. (e) Gibson, S. E.; Johnstone, C.; Loch, J. A.; Steed, J. W.; Stevenazzi, A. *Organometallics* **2003**, *22*, 5374. (f) van Rensburg, H.; Tooze, R. P.; Foster, D. F.; Slawin, A. M. Z. *Inorg. Chem.* **2004**, *43*, 2468.
- (4) Poyatos, M.; McNamara, W.; Incarvito, C.; Peris, E.; Crabtree, R. H. *Chem. Commun.* **2007**, 2267.
- (5) Kreisel, K. A.; Yap, G. P. A.; Theopold, K. H. *Chem. Commun.* **2007**, 1510; *Organometallics* **2006**, *25*, 4670.
- (6) (a) Zhang, X.; Xi, Z.; Liu, A.; Chen, W. *Organometallics* **2008**, *27*, 4401. (b) Ye, J.; Jin, S.; Chen, W.; Qiu, H. *Inorg. Chem. Commun.* **2008**, *11*, 404. (c) Zhang, X.; Xia, Q.; Chen, W. *Dalton Trans.* **2009**, 7045. (d) Sinha, A.; Rahaman, S. M. W.; Sarkar, M.; Saha, B.; Daw, P.; Bera, J. K. *Inorg. Chem.* **2009**, *48*, 11114. (e) Chang, Y.-H.; Liu, Z.-Y.; Liu, Y.-H.; Peng, S.-M.; Chen, J.-T.; Liu, S.-T. *Dalton Trans.* **2011**, 40, 489.
- (7) Chardon-Noblat, S.; Cripps, G. H.; Deronzier, A.; Field, J. S.; Gouws, S.; Haines, R. J.; Southway, F. *Organometallics* **2001**, *20*, 1668.
- (8) (a) Homanen, P.; Haukka, M.; Ahlgrén, M.; Pakkanen, T. A.; Baxter, P. N.W.; Benfield, R. E.; Connor, J. A. J. *Organomet. Chem.* **1998**, *552*, 205. (b) Haukka, M.; Kiviahio, J.; Ahlgrén, M.; Pakkanen, T. A. *Organometallics* **1995**, *14*, 825.
- (9) Bera, J. K.; Sadhukhan, N.; Majumdar, M. *Eur. J. Inorg. Chem.* **2009**, 4023, and references therein.
- (10) Patra, S. K.; Majumdar, M.; Bera, J. K. *J. Organomet. Chem.* **2006**, *691*, 4779.
- (11) (a) Li, C.; Widjaja, E.; Garland, M. J. *Am. Chem. Soc.* **2003**, *125*, 5540. (b) Li, C.; Chen, Li; Garland, M. J. *Am. Chem. Soc.* **2007**, *129*, 13327. (c) Roberts, J.; Lee, C. *Org. Lett.* **2005**, *7*, 2679. (d) Duschek, A.; Kirsch, S. F. *Angew. Chem., Int. Ed.* **2008**, *47*, 5703. (e) Jautze, S.; Peters, R. *Angew. Chem., Int. Ed.* **2008**, *47*, 9284. (f) Handa, S.; Nagawa, K.; Sohtome, Y.; Matsunaga, S.; Shibasaki, M. *Angew. Chem., Int. Ed.* **2008**, *47*, 3230. (g) Yoshikai, N.; Matsuda, H.; Nakamura, E. *J. Am. Chem. Soc.* **2009**, *131*, 9590. (h) Das, R. K.; Saha, B.; Rahaman, S. M. W.; Bera, J. K. *Chem.—Eur. J.* **2010**, *16*, 14459.
- (12) (a) Doyle, M. P. *Homogenous Transition Metal Catalysts in Organic Synthesis*; Moser, W. R.; Slocum, D. W., Eds.; ACS Advanced Chemistry Series No. 230; American Chemical Society: Washington, DC, 1992. (b) Taber, D. F. *Comprehensive Organic Synthesis*; Pattenden, G., Ed.; Pergamon Press: Oxford, UK, 1991; Vol. 3, p 1045. (c) Doyle, M. P.; McKervey, M. A.; Ye, T. *Modern Catalytic Methods for Organic Synthesis with Diazo Compounds*; John Wiley and Sons: New York, 1998. (d) Doyle, M. P. *Chem. Rev.* **1986**, *86*, 919. (e) Ye, T.; McKervey, M. A. *Chem. Rev.* **1994**, *94*, 1091. (f) Padwa, A.; Austin, D. J. *Angew. Chem., Int. Ed. Engl.* **1994**, *33*, 1797. (g) Doyle, M. P.; Forbes, D. C. *Chem. Rev.* **1998**, *98*, 911.
- (13) (a) Fructos, M. R.; Belderrain, T. R.; Nicasio, M. C.; Nolan, S. P.; Kaur, H.; Daz-Requejo, M. M.; Perez, P. J. *J. Am. Chem. Soc.* **2004**, *126*, 10846. (b) Fructos, M. R.; Belderrain, T. R.; Frémont, P. d.; Scott, N. M.; Nolan, S. P.; Díaz-Requejo, M. M.; Pérez, P. J. *Angew. Chem., Int. Ed.* **2005**, *44*, 5284. (c) Díaz-Requejo, M. M.; Pérez, P. J. *Chem. Rev.* **2008**, *108*, 3379.
- (14) (a) Maas, G. *Chem. Soc. Rev.* **2004**, *33*, 183. (b) Maas, G.; Werle, T.; Alt, M.; Mayer, D. *Tetrahedron* **1993**, *49*, 881. (c) Sevryugina, Y.; Weaver, B.; Hansen, J.; Thompson, J.; Davies, H. M. L.; Petrukhina, M. A. *Organometallics* **2008**, *27*, 1750.
- (15)  $^{31}\text{P}$  NMR (202 MHz,  $\text{CDCl}_3$ , 25 °C) experiment was performed with **1-BAr<sup>F</sup>**,  $\text{PPh}_3$ , and EDA in 1:1.2:1 ratio. Signals corresponding to cisoid and transoid isomers were found at  $\delta$  22.9 and 21.2 ppm, respectively.
- (16) An identical mechanism has been described for Fe(II)-porphyrin catalyst. See: Mirafzal, G. A.; Cheng, G.; Woo, L. K. *J. Am. Chem. Soc.* **2002**, *124*, 176.
- (17) Patra, S. K.; Bera, J. K. *Organometallics* **2006**, *25*, 6054.
- (18) Petrukhina, A.; Sevryugina, Y.; Andreini, K. W. *J. Cluster Sci.* **2004**, *15*, 451.
- (19) SAINT+ software for CCD diffractometers; Bruker AXS: Madison, WI, 2000.
- (20) Sheldrick, G. M. *SADABS Program for Correction of Area Detector Data*; University of Göttingen: Göttingen (Germany), 1999.
- (21) SHELXTL Package v. 6.10; Bruker AXS: Madison, WI, 2000. Sheldrick, G. M. *SHELXS-86* and *SHELXL-97*; University of Göttingen: Göttingen (Germany), 1997.
- (22) Spek, A. L. *PLATON*; University of Utrecht (The Netherlands), 2001.
- (23) Farrugia, L. J. *J. Appl. Crystallogr.* **1997**, *30*, 565.
- (24) Parr, R. G.; Yang, W. *Density-Functional Theory of Atoms and Molecules*; Oxford University Press: Oxford, U.K., 1989.
- (25) (a) Becke, A. D. *J. Chem. Phys.* **1993**, *98*, 5648. (b) Lee, C.; Yang, W.; Parr, R. G. *Phys. Rev. B* **1998**, *37*, 785.
- (26) (a) Hay, P. J.; Wadt, W. R. *J. Chem. Phys.* **1985**, *82*, 270. (b) Wadt, W. R.; Hay, P. J. *J. Chem. Phys.* **1985**, *82*, 284. (c) Hay, P. J.; Wadt, W. R. *J. Chem. Phys.* **1985**, *82*, 299.
- (27) Frisch, M. J.; Trucks, G. W.; Schlegel, H. B.; Scuseria, G. E.; Robb, M. A.; Cheeseman, J. R.; Montgomery, J. A., Jr.; Vreven, T.; Kudin, K. N.; Burant, J. C.; Millam, J. M.; Iyengar, S. S.; Tomasi, J.; Barone, V.; Mennucci, B.; Cossi, M.; Scalmani, G.; Rega, N.; Petersson, G. A.; Nakatsuji, H.; Hada, M.; Ehara, M.; Toyota, K.; Fukuda, R.; Hasegawa, J.; Ishida, M.; Nakajima, T.; Honda, Y.; Kitao, O.; Nakai, H.; Klene, M.; Li, X.; Knox, J. E.; Hratchian, H. P.; Cross, J. B.; Adamo, C.; Jaramillo, J.; Gomperts, R.; Stratmann, R. E.; Yazyev, O.; Austin, A. J.; Cammi, R.; Pomelli, C.; Ochterski, J. W.; Ayala, P. Y.; Morokuma, K.; Voth, G. A.; Salvador, P.; Dannenberg, J. J.; Zakrzewski, V. G.; Dapprich, S.; Daniels, A. D.; Strain, M. C.; Farkas, O.; Malick, D. K.; Rabuck, A. D.; Raghavachari, K.; Foresman, J. B.; Ortiz, J. V.; Cui, Q.; Baboul, A. G.; Clifford, S.; Cioslowski, J.; Stefanov, B. B.; Liu, G.; Liashenko, A.; Piskorz, P.; Komaromi, I.; Martin, R. L.; Fox, D. J.; Keith, T.; Al-Laham, M. A.; Peng, C. Y.; Nanayakkara, A.; Challacombe, M.; Gill, P. M. W.; Johnson, B.; Chen, W.; Wong, M. W.; Gonzalez, C.; Pople, J. A. *Gaussian 03*; Gaussian, Inc.: Pittsburgh, PA, 2003.
- (28) Reed, A. E.; Weinstock, R. B.; Weinhold, F. *J. Chem. Phys.* **1985**, *83*, 735.